Received: 12 May 2020 | Revised: 7 April 2021 | Accepted: 8 April 2021

DOI: 10.1002/glia.24009

GLIA

WILEY

RESEARCH ARTICLE

Microglia-mediated phagocytosis of apoptotic nuclei is impaired in the adult murine hippocampus after stroke

Max Rudolph[1] | Christian W. Schmeer[1] | Madlen Günther[1] | Florus Woitke[1] | Carolin Kathner-Schaffert[1] | Lina Karapetow[1] | Julia Lindner[1] | Thomas Lehmann[3] | Gustav Jirikowski[4] | Otto W. Witte[1] | Christoph Redecker[1,2] | Silke Keiner[1]

[1]Hans-Berger Department of Neurology, Jena University Hospital, Jena, Germany

[2]Department of Neurology, Lippe General Hospital, Lemgo, Germany

[3]Institute of Medical Statistics and Computer Science, University Hospital Jena, Friedrich Schiller University Jena, Jena, Germany

[4]Health and Medical University Potsdam, University Potsdam, Potsdam, Germany

Correspondence
Silke Keiner, Hans-Berger Department of Neurology, Jena University Hospital, Am Klinikum 1, 07747 Jena, Germany.
Email: silke.keiner@med.uni-jena.de

Funding information
Deutsche Forschungsgemeinschaft, Grant/Award Number: Ke1914/2-1; Else Kröner-Fresenius-Stiftung

Abstract

Following stroke, neuronal death takes place both in the infarct region and in brain areas distal to the lesion site including the hippocampus. The hippocampus is critically involved in learning and memory processes and continuously generates new neurons. Dysregulation of adult neurogenesis may be associated with cognitive decline after a stroke lesion. In particular, proliferation of precursor cells and the formation of new neurons are increased after lesion. Within the first week, many new precursor cells die during development. How dying precursors are removed from the hippocampus and to what extent phagocytosis takes place after stroke is still not clear. Here, we evaluated the effect of a prefrontal stroke lesion on the phagocytic activity of microglia in the dentate gyrus (DG) of the hippocampus. Three-months-old C57BL/6J mice were injected once with the proliferation marker BrdU (250 mg/kg) 6 hr after a middle cerebral artery occlusion or sham surgery. The number of apoptotic cells and the phagocytic capacity of the microglia were evaluated by means of immunohistochemistry, confocal microscopy, and 3D-reconstructions. We found a transient but significant increase in the number of apoptotic cells in the DG early after stroke, associated with impaired removal by microglia. Interestingly, phagocytosis of newly generated precursor cells was not affected. Our study shows that a prefrontal stroke lesion affects phagocytosis of apoptotic cells in the DG, a region distal to the lesion core. Whether disturbed phagocytosis might contribute to inflammatory- and maladaptive

Abbreviations: BrdU, Bromodeoxyuridine; CA1-CA3, cornu ammonis; DAPI, 4′,6-diamidino-2-phenylindole; DCX, doublecortin; H_2O_2, hydrogen peroxide; HCl, hydrochloric acid; Iba1, ionized calcium binding adaptor molecule 1; IqR, interquartile; MCAO, middle cerebral artery occlusion; Mdn, median; NDS, normal donkey serum; NSC, neural stem cells; SGZ, subgranular zone; SVZ, subventricular zone; TBS, tris buffer saline.

Max Rudolph and Christian W. Schmeer contributed equally to this study.

processes including cognitive impairment following stroke needs to be further investigated.

KEYWORDS
activated caspase 3, dentate gyrus, MCAO, neurogenesis, pyknotic cells

1 | INTRODUCTION

Epidemiologically, stroke is not only the main cause of disability in adulthood, but can also promote the long-term development of advanced epilepsy and dementia (Escobar et al., 2014; Zelano, 2019). Dementia often involves memory impairment associated with reduced ability to store new information, depending on the vascular territories affected. The hippocampal formation, lying deep in the medial temporal lobe is highly involved in memory formation (Bird & Burgess, 2008).

Furthermore, the dentate gyrus (DG) of the hippocampus formation is a region of active neurogenesis throughout lifetime (Toda, Parylak, Linker, & Gage, 2019), and adult neurogenesis plays a critical role in maintenance of hippocampal memory (Alam et al., 2018). Adult neurogenesis is present under physiological conditions as well as in a variety of neurological disorders such as epilepsy and stroke (Jessberger & Parent, 2015; Niv et al., 2012; Sierra et al., 2015; Woitke et al., 2017). In particular, a stroke lesion induces activation of stem cells within a short time and leads to an increased generation of neuronal precursors (Kunze et al., 2006; Walter, Keiner, Witte, & Redecker, 2011). This precursor population matures into neurons over several developmental stages. Consequently, stroke induces a massive increase in the formation of new neurons in the DG within the first 6 weeks post-infarction (Woitke et al., 2017). These post-stroke neurons are integrated into the existing neural network in the long term (Ceanga et al., 2019; Geibig, Keiner, & Redecker, 2012). In addition to the regularly integrated neurons, morphologically aberrant neurons could be detected (Bielefeld et al., 2019; Niv et al., 2012). The survival and integration of aberrant neurons is critical for the regular function of the existing neural network. Over time, however, stroke-induced neurogenesis strongly decreases, which is accompanied by cognitive deficits (Kathner-Schaffert et al., 2019).

The process of neurogenesis goes through two critical phases in which progenitor cells die. The first phase is the transition of neural precursor cells into the neuronal lineage. Progenitors that do not survive this transition become apoptotic and are phagocytized by the resident microglia within the first week of life (Sierra et al., 2010). This phagocytosis, already described under physiological conditions, is highly efficient and eliminates more than 90% of apoptotic progenitor cells. Phagocytosis represents an important regenerative process and is crucial for tissue homeostasis. Under inflammatory conditions, the phagocytic activity is increased (Abiega et al., 2016; Luo, Koyama, & Ikegaya, 2016; Sierra et al., 2010). In this context, microglia respond to apoptotic or dead cells such as progenitor populations and neurons by phagocytosis (Bessis, Bechade, Bernard, & Roumier, 2007). Interestingly, changes in phagocytic activity depend on the type of pathology. Induction of chronic epilepsy leads to a reduction in phagocytic microglial activity (Abiega et al., 2016). The persistence of non-phagocytized apoptotic cells can weaken the balance and may lead to an increase in the toxic intracellular response of the tissue and induce further inflammation. One of the critical functions of microglia in the brain is to engulf and remove dead cells or debris (Luo et al., 2016). This important function of microglia promotes the healthy balance of dying and living cells and also serves as a regulatory mechanism and adjusting screw for adult neurogenesis under physiological and pathophysiological conditions. After a stroke, there is an increase in both the number of apoptotic cells and the number of newly generated progenitor cells in the DG (Kim et al., 2015). In the present study, we tested the hypothesis that microglia have a limited capacity to take up and remove the dying and dead cells leading to their accumulation in the DG after stroke. The changes in phagocytic microglial activity after a prefrontal stroke have not been investigated yet and are the subject of our study. In the context of cell elimination, microglia appear to have a dual role. On the one hand, they remove apoptotic cells, described as caspase-3 positive cells, and their associated debris. On the other hand, they are themselves able to actively induce cell death of cells identified as caspase-negative (Sedel, Bechade, Vyas, & Triller, 2004; Wakselman et al., 2008). Microglia actively mediate cell death of both neurons and progenitor cells (Cunningham, Martinez-Cerdeno, & Noctor, 2013).

Here, we found a significant increase in the number of apoptotic cells within the first 2–4 days after stroke, including caspase-positive and -negative cells. While almost all apoptotic cells were phagocytized under sham conditions, the proportion of phagocytized cells after stroke was significantly decreased at Days 4 and 6 post stroke. The majority of apoptotic cells remaining in the DG were removed 10 days after lesion. This disturbed homeostasis might contribute to persistent neurogenesis and network alterations. Furthermore, such alterations could contribute to chronic cognitive deficits frequently observed after stroke (Brainin et al., 2015; Braun et al., 2017; Mijajlovic et al., 2017; Ojagbemi & Ffytche, 2016).

2 | MATERIALS AND METHODS

2.1 | Animals and experimental design

The study was performed on a total number of 60 adult, 12–13 weeks old C57BL/6J male mice. Animals were kept under standard conditions, on a 14 hr light/ 10 hr dark circle with free access to food and water. All mice received a single injection of BrdU 6 hr after MCAO or

sham surgery, followed by transcardial perfusion 1, 2, 4, 6 and 10 days postinfarct (Figure 1a). All animal procedures were approved by the local animal welfare committee and performed in accordance with the European Directives for the use of animals in experimental research.

2.2 | Cerebral ischemia model

Cerebral ischemia/reperfusion was induced in mice by MCAO, as previously described (Niv et al., 2012; Woitke et al., 2017). Mice were anesthetized with 2.5% isoflurane in a mixture of N_2O:O_2 (3:1). A midline-neck incision was performed to expose the right common carotid artery (CCA). The two bifurcations of the CCA, the external carotid artery (ECA) and the internal carotid artery (ICA), were localized and cleaned from surrounding tissue. The CCA and ECA were closed with a 7.0 polyfilament (Medicon eG, Tuttlingen, Germany). A 0.35 ± 0.02 mm diameter monofilament suture (Doccol Corporation, Sharon, MA) with a rounded tip was inserted into the ICA. The procedure leads to the occlusion of the middle cerebral artery. After 45 min of MCAO, the monofilament was removed, the ligature tightened and the wound closed. During MCA occlusion, mice body temperature was maintained using a heating pad. Sham-operated controls underwent surgery without occlusion of the middle cerebral artery and ligature of the common and the external carotid artery (Sieber et al., 2013; Woitke et al., 2017). According to the different survival periods after stroke, animals were assigned to five groups, each consisting of six MCAO and six sham mice. All mice survived the procedure and were included in the study.

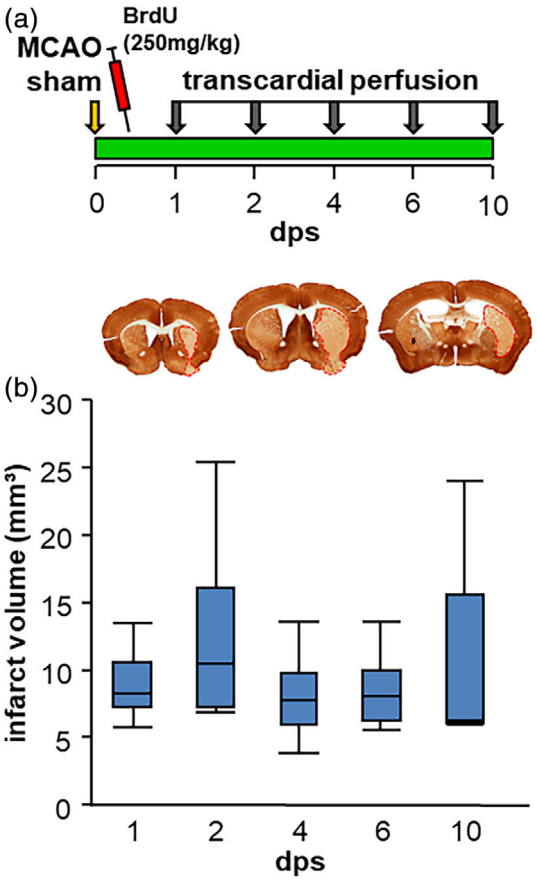

FIGURE 1 (a) Experimental design. Six hours after MCAO or sham surgery all mice received a single intraperitoneal injection of the proliferation marker BrdU. Mice were allowed to survive for 1, 2, 4, 6, and 10 days. (b) Representation of infarct volume using MAP2-stained brain slices. Red dotted lines mark the infarct core. There was no significant difference in the infarct volume between the different time points. All analyses were performed using the Mann–Whitney test; all median values, IQR and *p*-values are shown in Data S1. Box plot represents the median, upper and lower quartiles and min and max values. Scale bar: 1 mm. dps, day post stroke [Color figure can be viewed at wileyonlinelibrary.com]

2.3 | 5-Bromodeoxyuridine injections (BrdU)

Animals received a single intraperitoneal injection of BrdU (250 mg/kg body weight; Sigma Aldrich, St. Louis) dissolved in 0.9% saline 6 hr post-surgery, to label proliferating cells.

2.4 | Tissue preparation and immunohistochemistry

At 1, 2, 4, 6, or 10 days after surgery mice where deeply anesthetized and transcardially perfused to obtain brain tissue for immunohistochemistry (Keiner, Walter, Oberland, & Redecker, 2010). After transcardial perfusion, brains were removed and postfixed in 4% paraformaldehyde for 2 hr at room temperature. Fixed brains were cut into 50 μm serial coronal sections using a Vibrating Blade Microtome (Leica Biosystems, Newcastle, UK) and collected in Tris-buffered saline.

A peroxidase staining was performed on free floating brain sections in order to evaluate the total number of Ki67, BrdU, caspase-3, Iba-1 positive cells, or to determine the infarct volume (MAP2-staining). For the MAP2 staining every sixth brain section was selected and for BrdU, Ki67, activated caspase-3 and Iba1 every twelfth section was stained. Brain sections were incubated in 0.6% H_2O_2 for 30 min, rinsed three times in TBS for 15 min, and incubated in TBS containing 0.1% Triton, 3% NDS, 2% BSA, 3% slim milk (TBS-plus) and donkey IgG Fab fragment anti-mouse (1:200, Dianova, Hamburg, Germany) for 2 hr at room temperature. After washing three times with TBS for 15 min, sections were incubated in TBS with 3% NDS, 0.1% Triton and the mouse anti-MAP2 antibody (1:10,000; Sigma-Aldrich).

For BrdU staining, sections were placed in 2 N HCl for 30 min at 37°C followed by incubation with 0.1 N boric acid for 10 min. After washing twice with TBS for 15 min, slices were incubated in TBS-Plus for 30 min. Sections were then placed in TBS-plus and incubated with the primary antibody anti-rat BrdU, (1:500; Bio-Rad, Hercules).

Staining for activated caspase-3, Iba1 and Ki67 was performed in TBS-plus for 30 minutes and incubation with primary antibodies (anti rabbit activated caspase-3, 1:200; anti-rabbit Iba1, 1:500; anti rabbit Ki67, 1:500) overnight at 4°C.

On the next day, sections were washed with TBS three times for 15 min and then kept in TBS plus for 30 min. Thereafter, sections were incubated with secondary antibodies (IgG biotinylated anti mouse, 1:500, IgG biotinylated anti rat 1:500, IgG biotinylated anti rabbit, 1:500) in TBS-plus for 2 hr at room temperature. Sections were then washed with TBS three times for 10 min and placed in AB reagent (Vector Laboratories, Burlingame, CA) for 1 hr. After three washing steps with TBS for 15 min, sections were placed in 3,3′-Diaminobenzidine (DAB) solution (0.05 mg/ml TBS) and 0.03% H_2O_2 solution for 8 min. Following six washes with TBS for 10 min, sections were mounted with Entellan (Merck KGaA, Darmstadt, Germany).

2.5 | Immunofluorescence

Triple and quadruple immunofluorescence stainings using every twelfth serial section were performed to detect cell proliferation, apoptotic cells, neuronal precursors as well as phagocytosis, as previously described, using following primary antibodies: rat anti-BrdU (1:500; Bio-Rad, Hercules), rabbit anti-activated Caspase 3 (1:200; BD, Franklin Lakes), rabbit anti-Iba1 (1:500; Wako Chemicals GmbH, Neuss, Germany), guinea-pig anti-DCX (1:500, Merck KGaA, Darmstadt, Germany) and rabbit anti-Ki67 (1:500, Leica Biosystems, Newcastle, UK). Secondary antibodies used were: Alexa Fluor 488 anti-goat (1:500, Thermo Fisher Scientific Inc., Waltham), Alexa Fluor 488 anti-rabbit (1:500, Thermo Fisher Scientific Inc., Waltham), rhodamine anti-rabbit (1:500, Dianova, Hamburg, Deutschland), rhodamine anti-rat (1:500, Dianova, Hamburg, Deutschland), Cy5 anti-guinea pig (Dianova, Hamburg, Deutschland).

2.6 | Infarct volume

To determine brain and infarct volumes, brain sections stained for MAP2 were evaluated by means of digital image analysis. A previous study (Popp, Jaenisch, Witte, & Frahm, 2009) showed a higher sensitivity using MAP2 staining to clearly evaluate the infarct core and perilesional areas. The criterion for the detection of lesions was the absence of MAP2 immune reactivity, which was characterized by the loss of neurons. Images from every sixth brain slice were taken using a light table (Model B-95, Imaging Research Inc., St. Catharines, Canada), a digital camera (model C8484-05G, Hamamatsu Photonics KK, Hamamatsu, Japan) and the program SimplePCI (Version 6). Determination of the brain and infarct volumes was carried out with the image processing software Scion Image (Version 4). To determine the volumes, the area values were multiplied by the thickness of a single tissue section (50 μm) and the section interval value of six (Woitke et al., 2017).

2.7 | Cell quantification

Quantification of all cells was done by manual counting of the individual serial section, as the cells showed a good distribution in the tissue and overlapping could be excluded. Cell counting was conducted blinded by the experimenter.

2.7.1 | Number of BrdU, activated caspase-3, Iba1, and Ki67 positive cells

To determine the total number of BrdU-, activated caspase-3-, Iba1-, and Ki67-positive cells, we stained every 12th brain slice for DAB. Cell quantification was carried out with a light microscope (Zeiss Axioplan 2, Oberkochen, Germany) under ×40 magnification. All positive cells on the ipsilateral and contralateral sides to the lesion were counted. The two cell layers at the border to the hilus were considered as the subgranular zone. To determine the total number of cells, the values of the individual areas were taken and multiplied by 12.

2.7.2 | Number of DAPI positive apoptotic cells

To determine the number of apoptotic cells, DAPI stained cells were assessed on every 12th section. Apoptotic cells were identified by the rounding of the nucleus, a condensed chromatin and a reduction of the cell volume (Kroemer et al., 2009). To assess the total number of positive cells, results were multiplied by 12.

2.7.3 | Number of BrdU and DCX positive cells

Fluorescent signals of BrdU-DCX-positive cells were detected using a confocal laser scanning microscope (LSM 710 Meta, Carl Zeiss). Colocalization was confirmed by z-series through the cell soma allowing the definite assessment of overlap between the antigens. To assess the percentage of newly generated neuroblasts at the different time points, every 24th slices were used and the phenotypes of BrdU-positive cells per animal were determined bilaterally in the SGZ.

2.7.4 | Phagocytosis of Iba1-DAPI, BrdU, and DCX or NeuN positive cells

Three-dimensional confocal images of all Iba1/DAPI pyknotic nuclei, Iba1/DAPI/BrdU and Iba1/DAPI/BrdU/DCX stained slices were acquired and analyzed using the ZEN 2008 software (Carl Zeiss, Oberkochen, Germany). The evaluation was carried out in two steps: (a) DAPI pyknotic cell nuclei were considered as phagocytized and quantified if they were completely encapsulated by Iba1-positive microglia; (b) The pyknotic DAPI nucleus was phenotyped evaluating BrdU and/or DCX expression.

2.8 | Three-Dimensional reconstructions of pyknotic DAPI nuclei

To evaluate the phagocytosis of pyknotic nuclei, reconstructed 3D images were analyzed with the Amira® software (Version 4, Thermo Fisher Scientific Inc., Waltham). Cells were separately marked in the different channels for Iba1, DAPI, BrdU or DCX, and a 3D

reconstruction of them was created. The percentage of phagocytic co-labeled DAPI-positive cells was then calculated.

2.9 | 3D-Sholl analysis

The complexity of Iba1-stained microglia was quantitated by means of a Sholl analysis (McGill et al., 2018). A minimum of 220 individual microglia cells from each group in 40 μm thick sections were identified after immunofluorescence staining for Iba1. Z-stacks of Iba1-positive cells were performed in the DG and a Sholl analysis was carried out by using the Imaris software (Version 9.1.2, Bitplane, Belfast, NIR, UK). The interval between concentric circles was 1 μm with the center point at the soma.

2.10 | Statistical analysis

Statistical data analysis was performed using Mann–Whitney *U* test due to their skewed distribution. Median (Mdn) as well as interquartile range (IQR) are reported for each group (Data S1). In this exploratory analysis, each p value represented the level of evidence against each null hypothesis.

Sholl analysis of microglia was tested using the one-way ANOVA (dependent variable: intersections; factor: groups sham versus MCAO) with a Bonferroni post-hoc test at the different time points. The data are reported as mean ± *SEM*.

All statistical analyses were performed using SPSS 22.0 for Windows (IBM Corp., Armonk, NY). A p value of <.05 was considered to be statistically significant.

2.11 | Data availability

Data available in article Data S1.

3 | RESULTS

For a complete list of results (median, IQR, and p-values) see "Data S1."

3.1 | Brain infarct volumes

All animals showed a striatal infarct typical of MCAO. In all animals, the DG showed no evident damage (Figure 1b). Control mice did not show structural changes after the sham surgery. There were no significant differences between the infarct volumes within the different groups up to 10 days after stroke (Figure 1b; Data S1).

As expected, the striatum of animals from the stroke group exhibited tissue damage and cell loss after the MCAO.

3.2 | Quantification and distribution of DAPI-positive apoptotic cells

For the determination of apoptotic cells, DAPI stained pyknotic cell nuclei (Figure 2a/d) and activated caspase-3-positive cells (Figure 2f) were quantified in the DG. On Day 2 after stroke, the number of pyknotic, DAPI positive cells in the MCAO group was significantly increased compared with controls (p = .009; Figure 2b). This number decreased significantly between Day 2 and Day 4 in the MCAO group and reached the control level. The number of pyknotic DAPI-positive cells in the sham group did not significantly change over time. Analysis of the ipsi- and contralateral sides showed no significant differences between the MCAO and sham-operated groups (Figure 2c).

The DAPI pyknotic cells were detected in both the SGZ and the GCL (Figure 2d). In the GCL the number of pyknotic DAPI positive nuclei significantly increased at Day 2 (p = .002), Day 4 (p = .002), and Day 10 (p = .004) post infarct (Figure 2e). In particular, after stroke the number of pyknotic nuclei increased from Day 1 to Day 2 (Data S1). This increase in the number of pyknotic nuclei was significant at Days 2 and 10 compared to controls. No significant differences were observed in the sham operated groups from Day 1 to Day 10 (Data S1).

The number of activated caspase-3-positive cells was significantly increased at Day 4 in the stroke group compared to the sham group (p = .041; Figure 2g; Data S1). The caspase-3-positive cell sub-population represent a relevant fraction of the total number of apoptotic cells found. In addition, we show that this sub-population of apoptotic cells is actively phagocytized by microglia, as indicated by their engulfment (Figure 2f).

These results indicate that stroke induces cell death in the DG, as indicated by increased numbers of pyknotic cells up to Day 10 post-lesion. In addition, the data show that on Day 2 more caspase-negative cells are phagocytized, which indicates an active microglia-mediated cell death. This process shifts on Day 4, where a large proportion of the pyknotic cells are caspase-positive.

3.3 | Microglia in the dentate gyrus

To verify phagocytosis of apoptotic cells and microglia activity, microglia were first analyzed morphologically (Figure 3). Immunofluorescence labeling with antibodies against Iba1 and CD68 was used to characterize the activation state of microglia (Figure 3a/b). CD68 staining revealed high expression of microglia in the hilar region and partially in the DG, showing an enlarged soma after MCAO, which is a typical morphological response of activated microglia (Figure 3b). More detailed analysis was performed using Iba1 staining for accurate detection of the fine extensions of microglia. Morphological analysis showed a decrease in morphology on Days 1, 2, and 6 post-ischemic compared to the sham group (Figure 3c/d/f; Data S1). On Days 4 and 10, no significant differences were detected between MCAO and sham control (Figure 3e/g). The analyses thus showed post-stroke

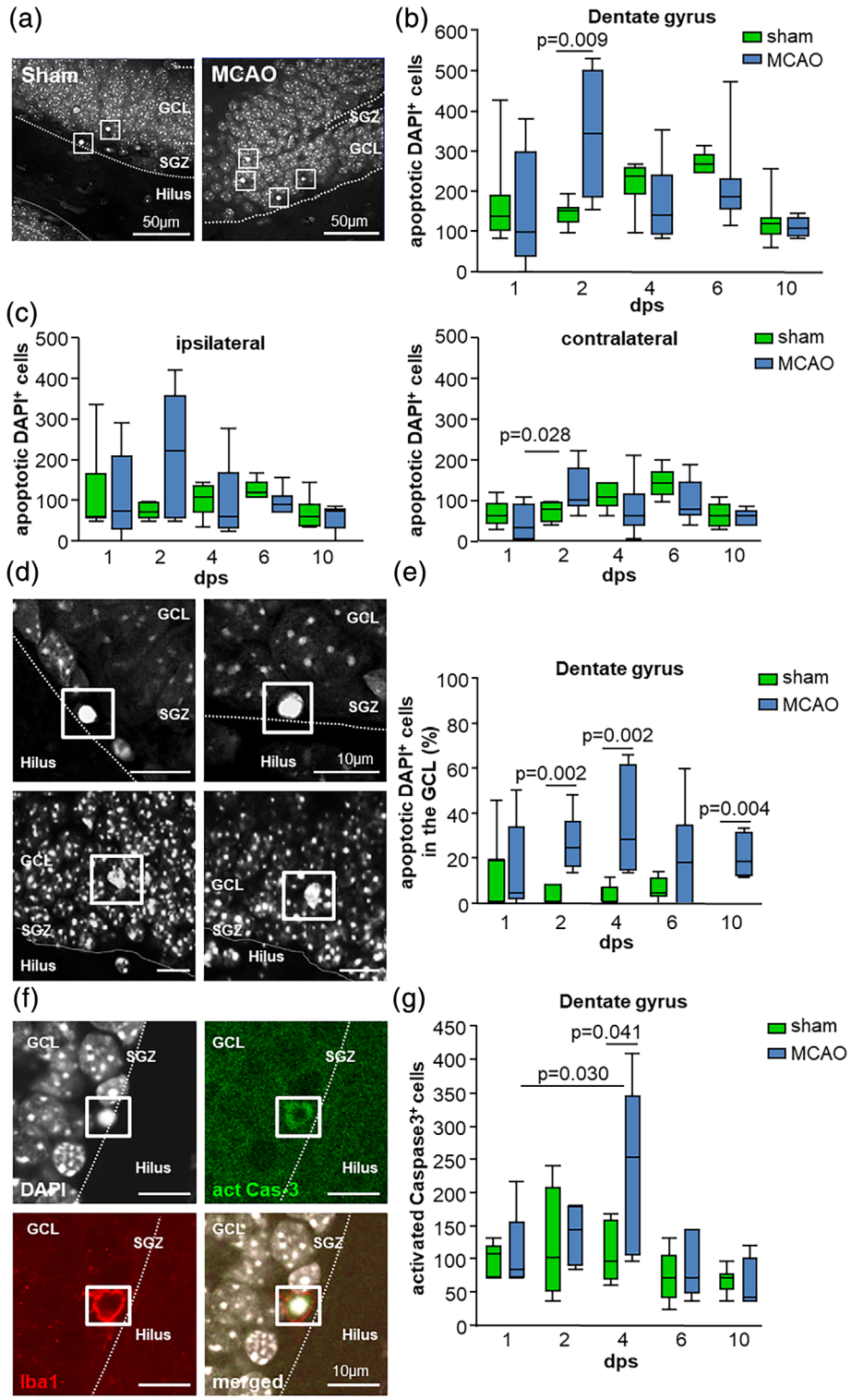

FIGURE 2 Apoptotic cells after infarct induction. (a) Images show apoptotic peroxidase-stained cells in the dentate gyrus of sham controls and MCAO group in the dentate gyrus. (b) Quantification of DAPI-positive apoptotic cells in the dentate gyrus. A significant increase in the number of DAPI-positive cells compared to sham animals was detected at Day 2 after stroke. (c) Analyses of the ipsi- and contralateral sides showed no significant changes between the sham and MCAO groups at the different time points. (d) The DAPI-positive nuclei were located in both the SGZ and GCL of the hippocampal dentate gyrus. The apoptotic cells were identified by small and bright shining nuclei. (e) Distribution of pyknotic DAPI-positive cells in the GCL of the dentate gyrus. After stroke the ratio of apoptotic cells was significantly increased in the GCL at Days 2, 4, and 10 post-stroke compared to sham animals. (f) Representative co-localization of activated caspase-3 and DAPI in a pyknotic cell. The depicted cell has been phagocytized by Iba1-positive microglia in the SGZ. (g) Total number of DAPI-activated-caspase-3 positive cells. Stroke significantly increased the caspase-3 activated cells 4 days after infarct induction. All analyses were performed using the Mann–Whitney test; all median values, IQR and *p*-values are shown in Data S1. Box plot represents the median, upper and lower quartiles and min and max values. dps, day post stroke [Color figure can be viewed at wileyonlinelibrary.com]

activation of microglia in the DG by partial expression of CD68 and reduced ramification.

In order to determine the phagocytic capacity of microglia to remove apoptotic cells and cell debris, we focused on Days 4 and 6 for further analysis, which include a high number of caspase-3-positive cells. Immunohistochemical staining of Iba1-positive microglia showed an even distribution of microglia in the sham- versus MCAO mice (Figure 4a1–4). Quantification of microglia indicated no significant differences in the number of Iba1-positive microglial cells in the DG of control and lesioned brains on Days 4 (p = .18) and 6 (p = .052) (Figure 4b) after surgery. The analysis of the ipsi- and contralateral sides also showed no significant differences between both regions (Figure 4c; Data S1).

There were no significant differences in the total number of microglia between the groups.

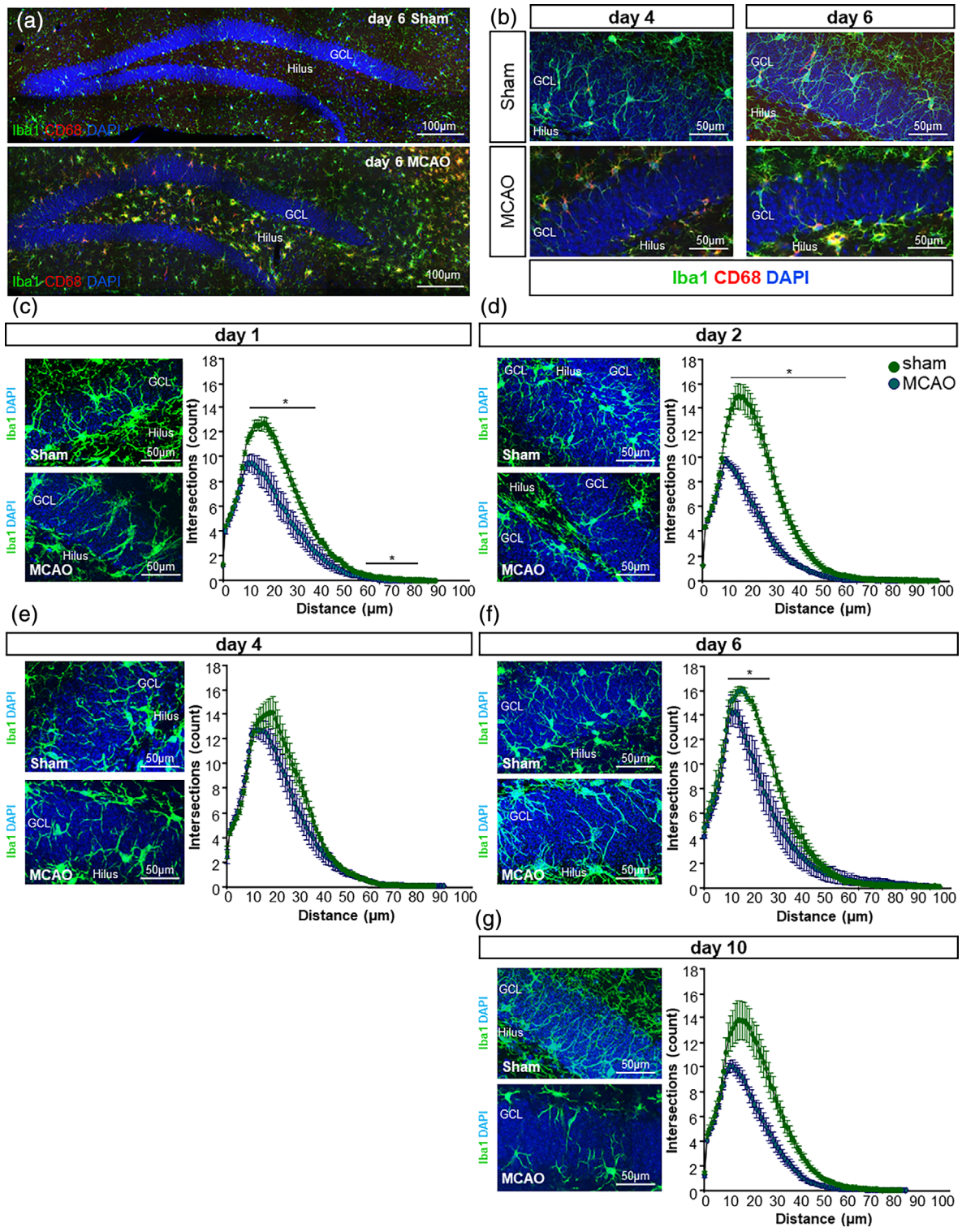

FIGURE 3 Microglia complexity after ischemic induction. (a) Overview image of the dentate gyrus in controls and stroke mice. Maximum projection of confocal z-stacks stained against Iba1, CD68, and DAPI. (b) The images show parts of the dentate gyrus under control and infarct conditions. The z-stacks were used for the Sholl analysis to verify the complexity of the microglia after stroke. (c–g) Sholl analysis of microglia complexity revealed changes at Days 1, 2, and 6. The graphs represent the means ± *SEM* using one-way ANOVA, $^*p < .05$ [Color figure can be viewed at wileyonlinelibrary.com]

3.4 | Phagocytic activity of microglia in the dentate gyrus after lesion

Quantification of phagocytized DAPI positive pyknotic cell nuclei was carried out by analysis of confocal images (Figure 5a1–4) and 3D reconstruction of engulfed apoptotic DAPI-positive nuclei by Iba1-positive microglia (Figure 5b1–2). We defined phagocytized cell nuclei as those completely encapsulated by the extensions of the microglia. The ratio of phagocytic microglia to the total number of microglia was markedly reduced after stroke at Day 4 (p = .041) and highly diminished at Day 6 after lesion (p = .008; Figure 5c). Quantification on the ipsilateral side showed a significant decrease in microglia that were phagocytically active on Day 6 (p = .032). On the contralateral side, significant differences were detected on Days 4 (p = .009) and 6 (p = .008) compared to the sham mice (Figure 5d). We also determined the ratio of the number of phagocytic microglia to the number of apoptotic cells and found it also to be significantly reduced (p = .041) at Day 4 post-lesion (Figure 5e). The percentage of apoptotic DAPI-positive cells on the contralateral side to the lesion was markedly reduced 6 days (p = .026) after infarct induction (Figure 5f).

In addition, we also determined the number of apoptotic nuclei per microglia (Figure 6a). While no differences were detected between the groups at Day 4, the MCAO animals showed a significant decrease in microglial phagocytosis of apoptotic cells at Day 6 (p = .03). We found up to two pyknotic DAPI positive nuclei in some microglia cells (Figure 6b), however, the number of apoptotic nuclei per microglia in the phagocytic cells was not changed due to the lesion (Data S1). We also evaluated the impact of the distal stroke lesion on the microglial capacity to phagocytize immature (DAPI-DCX$^+$) neurons (Figure 6c). No significant differences were observed in the number of phagocytized DCX positive cells (Data S1).

These results indicate that the number of phagocytic microglia was reduced following lesion, however, the phagocytic capacity of the microglia to engulf apoptotic cells remained unchanged. The number of phagocytized immature neurons did not change over time.

3.5 | Endogenous cell proliferation after stroke

In addition to apoptotic processes, we aimed to assess endogenous proliferation after stroke, and to what extent the balance between cell

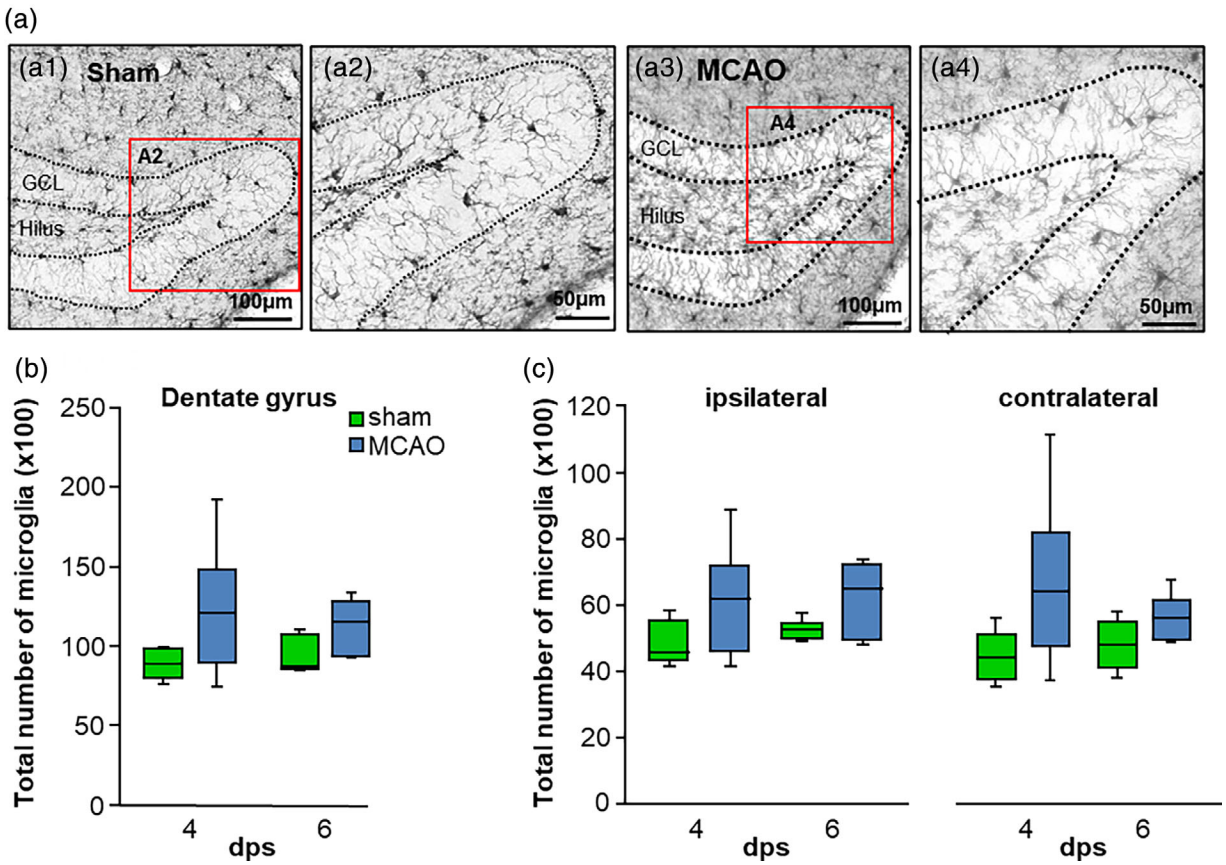

FIGURE 4 Quantification of the microglia. (a1–4) Images of Iba1 positive microglia in the dentate gyrus 4 days after stroke induction. (a2/a4) Higher magnification of the Iba1-positive microglia marked with rectangles in a1/a3. (b) The number of microglia was not changed after stroke compared to sham controls. (c) Detailed analyses of the ipsi- and contralateral sides showed no differences in the total number of microglia between the groups within the time points. Analyses were performed using the Mann–Whitney test; all median, IQR and p-values are shown in Data S1. dps, day post stroke [Color figure can be viewed at wileyonlinelibrary.com]

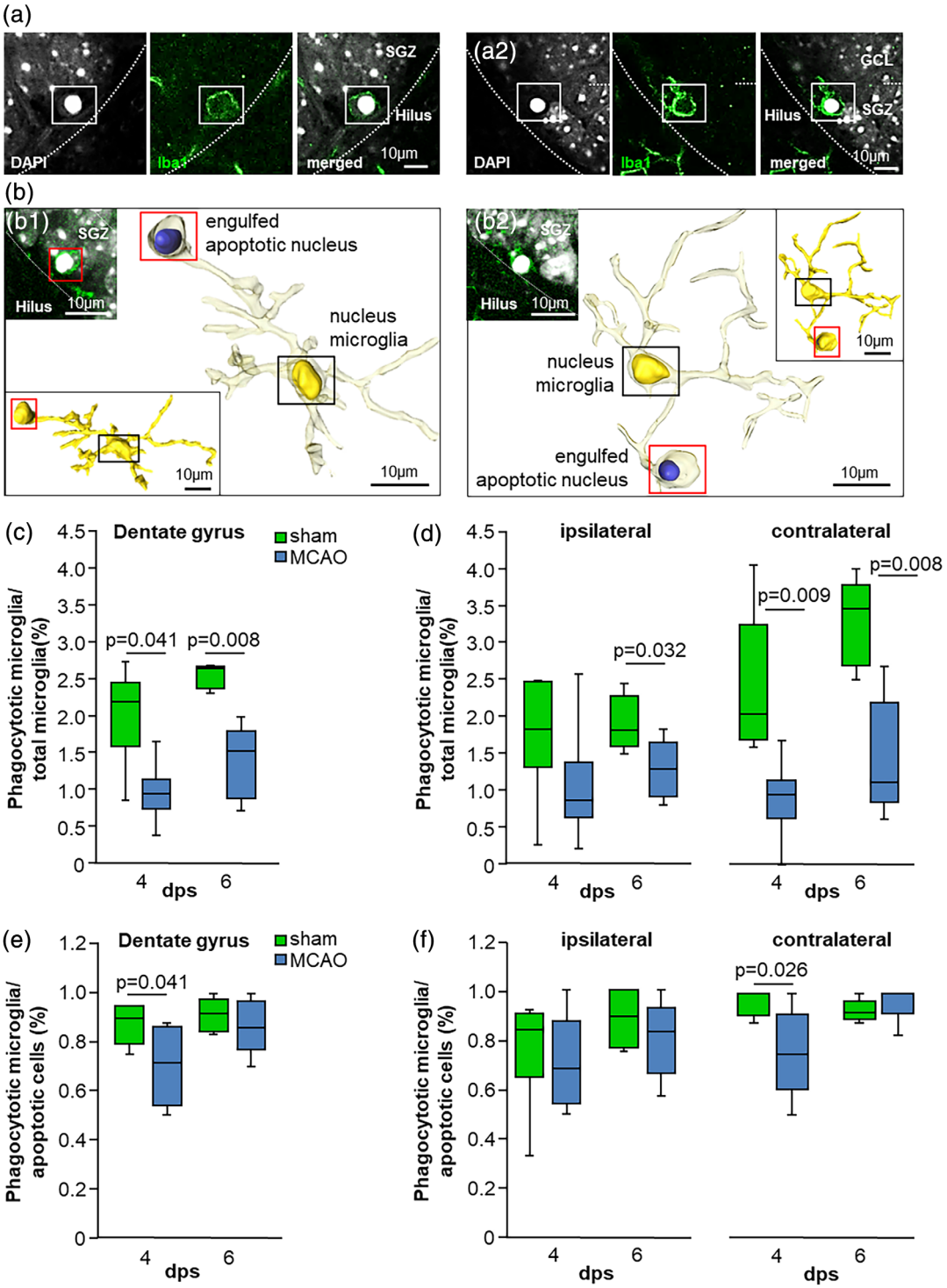

FIGURE 5 Phagocytosis of apoptotic cells by Iba1-positive microglia. (a1/a2) Confocal images of apoptotic DAPI-positive cells engulfed by microglia. (b1/b2) AMIRA 3D-reconstructions showing engulfed apoptotic DAPI positive cells by Iba1 positive microglia. Confocal image of the engulfed apoptotic cell (upper left). 3D reconstructions of microglia phagocytosis (upper right). Transparent 3D reconstruction showing engulfed apoptotic cell and microglia with nuclei. (c) The ratio of phagocytic active microglia to the total number of microglia. Phagocytosis was significantly reduced at Days 4 and 6 after stroke. (d) In comparison, phagocytosis was significantly decreased at Day 6 and contralateral at Days 4 and 6. (e) The ratio of phagocytotic microglia to all pyknotic DAPI positive cells was significantly reduced in the dentate gyrus of the infarct group compared to sham on Day 4 after lesion. (f) The reduction of phagocytic microglia was observed at the contralateral side. All analyses were performed using the Mann–Whitney test; all median, IQR and *p*-values are shown in Data S1. Box plot represents the median, upper and lower quartiles and min and max values. dps, day post stroke [Color figure can be viewed at wileyonlinelibrary.com]

renewal and death was changed. To assess endogenous proliferation of progenitor cells in the DG after stroke, Ki67-positive cells were quantified (Figure 7a). Within the stroke groups there was a significant increase in cell number starting on Day 1 (p = .009). From Day 4 up to Day 10 the cell number returned to baseline (p = .017). Cell numbers in the stroke group were significantly increased compared to the control group on Day 4 (p = .015). The control groups showed a stable number of Ki67 positive cells at the different time points (Figure 7b; Data S1). No significant changes were observed in the SGZ on the ipsilateral side, but there was a significant increase in Ki67-positive cells on the contralateral side on Day 4 (Figure 7c).

Interestingly, the highest proliferation rate occurred on Day 4, which was associated with a significant increase in apoptotic caspase-3-positive cells. These findings may suggest that there is a balance between cell generation and depletion.

3.6 | Microglia-mediated phagocytosis of newly generated pyknotic cells

In the DG, new neurons are continuously generated throughout adulthood. This requires the proliferation of neural precursor cells. It has been shown that proliferation of neural precursor cells is increased after MCAO. However, the effect of stroke on the rate of generation and elimination of these precursor cells after lesion has not yet been examined. Furthermore, whether microglia-mediated phagocytosis of newly generated apoptotic cells is altered after stroke is currently unknown.

Within the sham group, there was no significant change in the number of BrdU-positive cells from Day 1 to Day 4 (Figure 8a/b). From Day 4 to Day 6, this value then dropped significantly by 47.4% to Mdn 1,668 cells (p = .002) and remained significantly reduced until Day 10 (p = .009). Within the MCAO group, there was an increase in the number of BrdU-positive cells up to Day 6, which became significant from Day 1 to Day 2 (p = .004). There was also a significant difference in the number of cells between the infarct and sham groups on Day 1 (p = .026) and on Day 6 (p = .009). In contrast to the sham group, the number of cells in the MCAO group remained at twice the level on Day 6. At Day 10, the number of BrdU-positive cells in the MCAO group was significantly reduced as compared to Day 6 (p = .002) and similar to the corresponding sham group (p = .093; Figure 8b). At Day 10, the number of BrdU-positive cells in both sham and MCAO groups was significantly lower as compared to Day 1. Separate analysis of the ipsi- (p = .026) and contralateral (p = .004) side showed a bilateral significant increase in BrdU-positive cells on Day 6 post-lesion (Figure 8c). Thus, the stroke increased the number of BrdU-positive cells in the DG on both sides.

BrdU-positive cells were analyzed for co-expression of the neuronal marker DCX (Figure 8d). At all-time points, the percentage of BrdU/DCX-positive cells did not differ between the groups (Figure 8e).

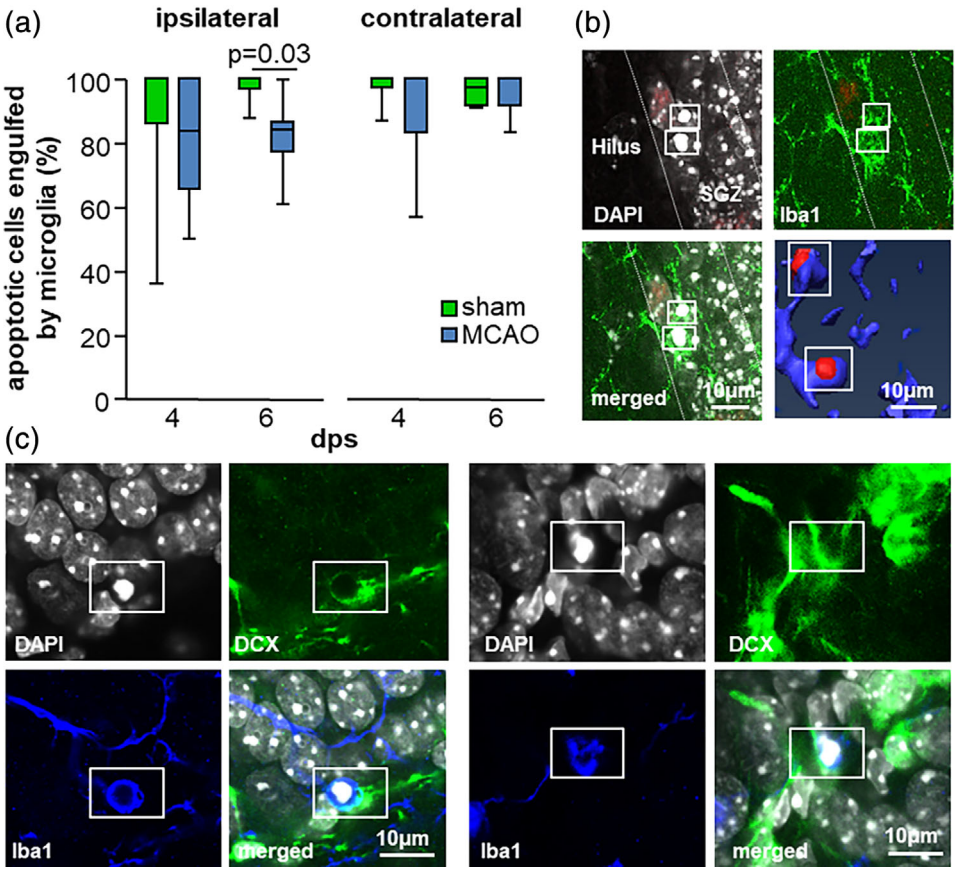

FIGURE 6 Microglia engulfment. (a) Percentage of apoptotic DAPI-positive cells engulfed by microglia. After stroke the number of engulfed apoptotic cells significantly decreased in the ipsilateral hemisphere at Day 6. (b) Confocal images represent microglia, which simultaneously phagocytized two pyknotic DAPI-positive cells. AMIRA 3D-reconstruction show microglia with two engulfed apoptotic cells. There was no difference in the phagocytic profile of microglia between sham and MCAO groups on Days 4 and 6 after stroke. (c) Confocal images show phagocytic immature DCX-positive neurons. All analyses were performed using the Mann–Whitney test; all median, IQR and p-values are shown in Data S1. Box plot represents the median, upper and lower quartiles and min and max values. dps, day post stroke [Color figure can be viewed at wileyonlinelibrary.com]

We also determined the ratio between the number of apoptotic DAPI-BrdU-positive cells and the number of newly generated cells in the DG (Figure 8f1/2). The ratio of BrdU-pyknotic cells was significantly increased in the MCAO compared to the sham group (p = .009) in the ipsilateral hemispheres at Day 4 post infarct (Figure 8g). There was no difference in the capacity of microglia in the different groups to engulf apoptotic cells (Data S1).

Here we found an increased cell survival, as indicated by a higher number of BrdU-positive cells up to Day 6 after lesion. At Day 10, there was no significant difference between sham and MCAO animals.

4 | DISCUSSION

In the present study, we found that a prefrontal stroke lesion partially activates microglia in the distal DG of the hippocampal formation. Despite their activation state, microglial phagocytic activity was impaired, leading to an increase in the number of caspase-3 positive apoptotic cells, which occurred more frequently in the granule cell layer after stroke. The increased number of caspase-3 positive cells suggests that microglia mainly remove cells that are already on their way to die. Phagocytized apoptotic cells included only a few immature apoptotic neurons. Interestingly, we also found that the increased number of non-phagocytized apoptotic cells did not alter the total number of microglial cells after lesion. Moreover, we observed a brief increase in endogenous cell proliferation at the time point of the highest number of caspase-3 positive apoptotic cells. The newly-formed BrdU positive cells exhibited a prolonged survival after stroke.

4.1 | Microglial phagocytic activity is reduced after stroke in the hippocampus

Microglia are necessary to remove dead cells and thus maintain tissue homeostasis. After stroke, the phagocytosis-mediated removal of apoptotic cells was significantly reduced at the peak of cell death after lesion. However, the phagocytic capacity of active microglia, in terms of the number of apoptotic cells phagocytized per cell, was not affected after stroke induction. We found that under control conditions, phagocytosis of apoptotic cells by microglia was more than 90%. These results are consistent with the studies by Sierra et al. (2010). Using mice of different ages, they showed that microglia carry out continuous and efficient phagocytosis in the subgranular zone, and found that more than 90% of newly generated cells were

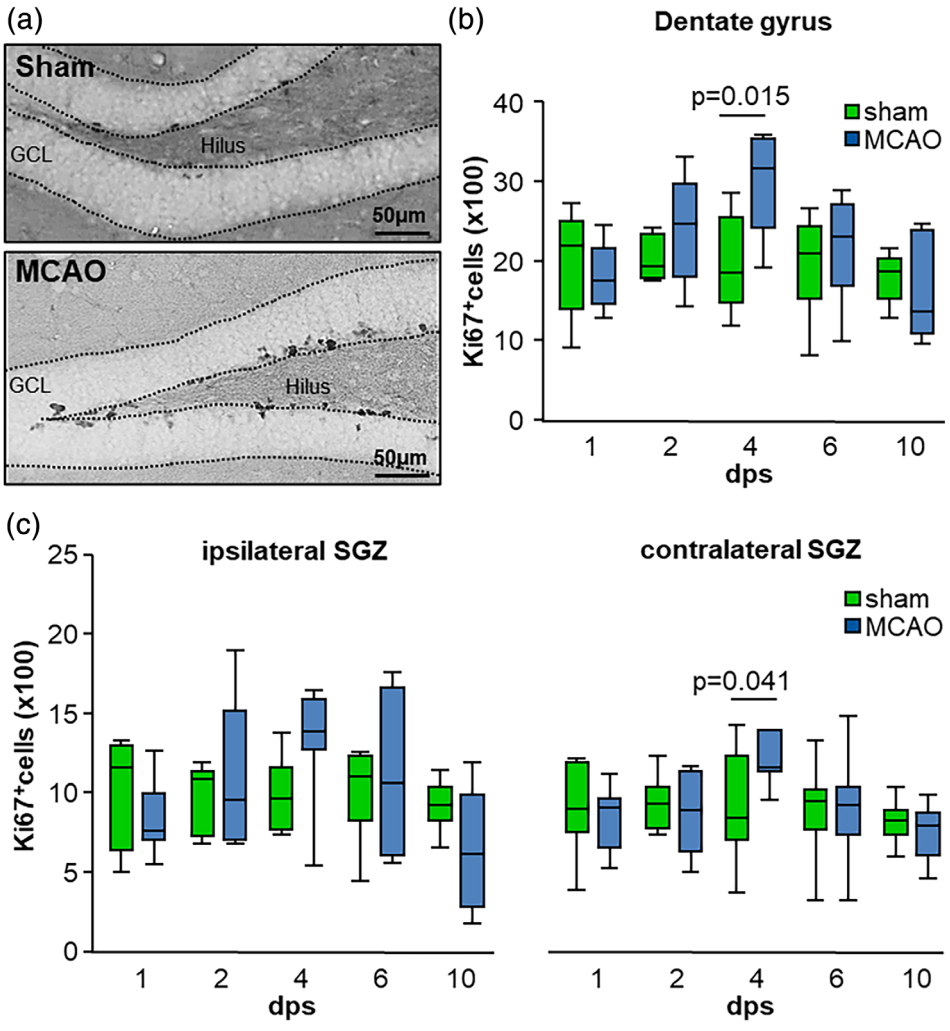

FIGURE 7 Quantification of endogenous proliferation after stroke. (a) Images of sections from the dentate gyrus after peroxidase-staining to evaluate the total number of Ki67-positive cells in sham controls and MCAO mice. (b) Total number of Ki67-positive cells in the dentate gyrus at the different time points post-surgery. The number of proliferating Ki67-positive cells increased from Day 1 to Day 4 after MCAO, followed by a decrease from Day 4 to Day 10. Significant differences between the groups were observed at Day 4. (c) Significant differences were detected on the contralateral side at Day 4. All analyses were performed using the Mann–Whitney test; all median, IQR and p-values are shown in Data S1. Box plot represents the median, upper and lower quartiles and min and max values. dps, day post stroke [Color figure can be viewed at wileyonlinelibrary.com]

phagocytized. Non-phagocytized cells were always in contact with a microglial process at the beginning of phagocytosis. It was, therefore, assumed that all apoptotic cells in the brain were phagocytized (Sierra et al., 2010). This high phagocytic activity under physiological conditions leads to the conclusion that the microglia are intensively involved in homeostasis and that the neural networks are not disturbed by their activity.

In contrast to the high efficiency of microglial phagocytosis under control conditions, the present study shows a strong decrease in phagocytosis after stroke. A previous study (Abiega et al., 2016) showed that pathological changes differently affect microglial activity. Acute inflammation with LPS was shown to increase the number of apoptotic cells and phagocytic activity of microglia within the first 8 hr, while the number of microglia remained stable. Following chronic

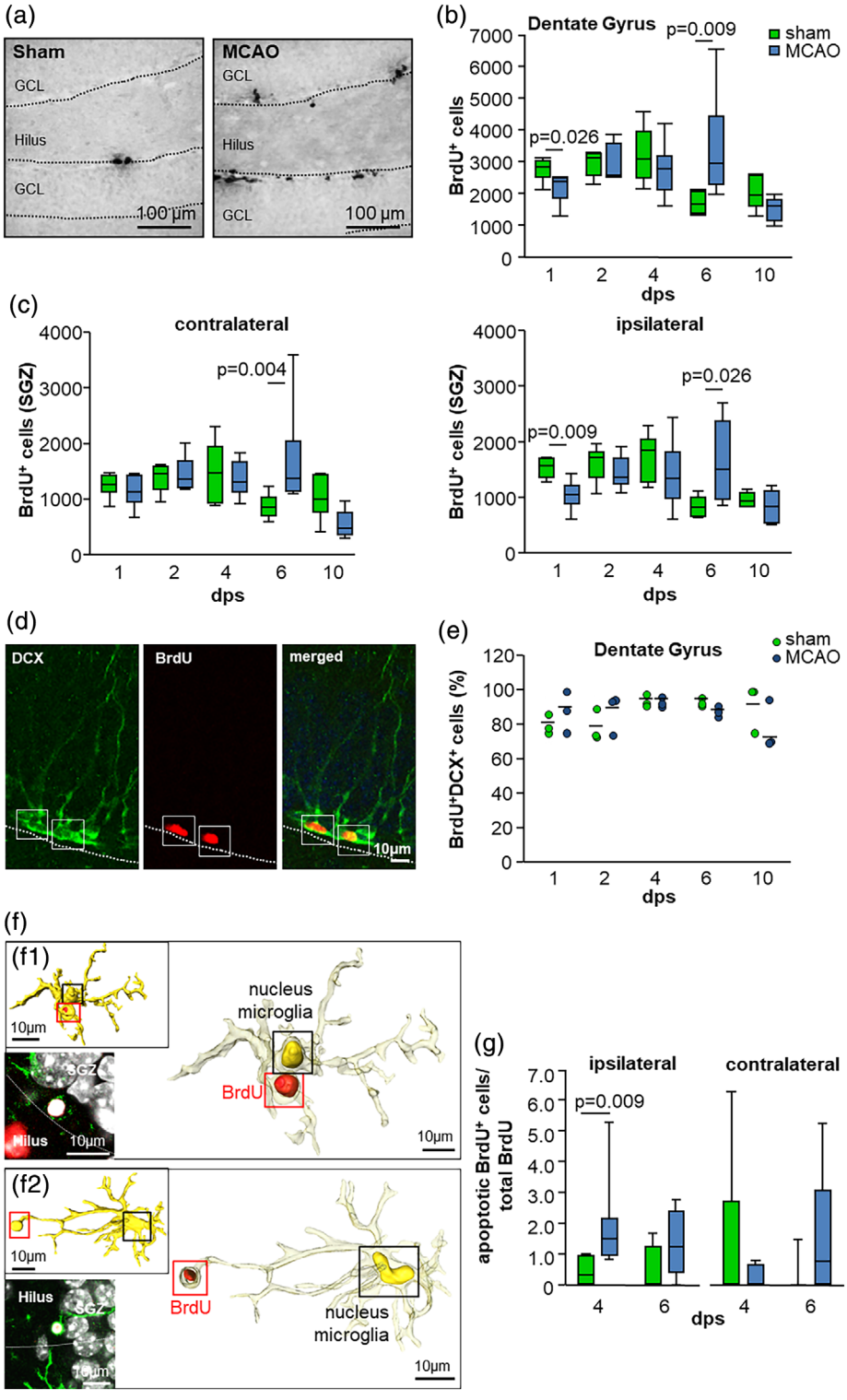

FIGURE 8 Quantification of BrdU positive cells. (a) Images of sections from the dentate gyrus after peroxidase-staining to localize BrdU at Day 6 post infarction. (b) Stroke significantly increased the number of BrdU positive cells 6 days after surgery compared to sham controls. (c) The total number of BrdU-positive cells was significantly increased in the ipsi- and contralateral side on Day 6 after MCAO. (d) Confocal images of immunofluorescent sections for doublecortin (DCX), BrdU and merged. (e) No differences in the total number of newly-generated immature neurons were observed between both groups. (f) Two representative images (f1/f2) showing 3D-reconstructions of BrdU positive cells (red) engulfed by microglia (light yellow/transparent; nuclei yellow). Insert top left is the external view of the microglial cell. Insert bottom left is the confocal image of the reconstructed BrdU pyknotic cell. (g) The ratio of apoptotic BrdU-positive cells to the total number of BrdU positive cells was significantly increased in the ipsilateral side on Day 4 after MCAO. All analyses were performed using the Mann–Whitney test; all median, IQR and p-values are shown in Data S1. Box plot represents the median, upper and lower quartiles and min and max values. dps, day post stroke [Color figure can be viewed at wileyonlinelibrary.com]

inflammation, an increase in apoptosis and microglia was demonstrated. After both acute and chronic inflammation, maintenance of phagocytosis/apoptosis ratios was granted, so that phagocytosis of apoptotic cells was unaffected. In contrast, after an epileptic seizure the number of apoptotic cells increases strongly, but the phagocytosis of these cells decreases massively. Importantly, in both cases the number of microglia remained constant. In addition to the constant number of microglia up to Day 1 post induction of epilepsy, Luo et al. (2016) found an increase of microglia on Day 6, which was accompanied by an increase of CD68 expression in the microglia. Interestingly, activated microglia mainly enclosed caspase negative non-apoptotic cells (Luo et al., 2016). Similarly as for the study by Luo et al. (2016), we found an impaired uptake of apoptotic cells by a constant number of microglia. The different models of inflammation, epileptic seizure or stroke indicate different microglial strategies to deal with increasing numbers of apoptotic cells. Microglia can increase their uptake capacity of apoptotic cells or more microglia become phagocytically active in order to remove dead cells. Furthermore, phagocytosis can also be increased by a single microglial taking up several apoptotic cells simultaneously. However, none of these strategies necessarily leads to an increase in the total number of microglia (Abiega et al., 2016). The fact that we did not observe an increased uptake of multiple apoptotic cells by microglia might be explained by the spatial distribution of the apoptotic cells within the DG. The apoptotic cells mostly occurred individually and not in clusters, so that simultaneous phagocytosis of multiple apoptotic cells by single microglia was not possible.

Overall, there was a reduction in the phagocytotic efficiency of microglia in the stroke group, particularly on Day 4 such that increased caspase-3 positive apoptotic cells remained and were not phagocytized. To what extent the heterogeneity of apoptotic cells plays a role in phagocytosis as well as the possible signaling pathways involved are not yet clear. Such a disturbance has so far only been demonstrated in a temporal lobe epilepsy model (Abiega et al., 2016; Palomba et al., 2021; Sierra-Torre et al., 2020). In this model, the epileptogenic overexcitation resulted in a strong release of ATP from neurons and astrocytes. Similar to excessive background noise, this ATP release overlapped the ATP gradient emanating from apoptotic cells, which serves the microglia to detect cells to be phagocytized ("find-me" signal; Abiega et al., 2016; Dale & Frenguelli, 2009; Santiago et al., 2011). A previous study showed a hypoxically induced increase in the release of glutamate with subsequent increase of intracellular and extracellular ATP release, which was also demonstrated during stroke (Melani et al., 2005).

4.2 | Impaired microglial phagocytosis does not affect newly formed cells

Importantly, although we found a reduced microglia-mediated phagocytosis, it did not equally affect all apopotic cell populations. In particular, elimination of newly formed BrdU-positive cells after stroke was not impaired. It is unclear whether there are differences between the apoptotic BrdU-positive cells and the non-newly formed cells. Furthermore, to what extent altered signaling pathways like ATP gradients cause the reduction in phagocytotic activity and the significance of other "find-me" signaling molecules requires further investigation.

Regardless of the cause for the reduced phagocytic activity, this in combination with an increased number of apoptotic cells has various potential consequences including an increase in the risk of a local inflammatory reaction. Reduced phagocytosis is in itself pro-inflammatory, since during phagocytosis there is already a release of anti-inflammatory messenger substances and a reduced release of proinflammatory molecules (Chan, Magnus, & Gold, 2001; Savill & Fadok, 2000). Furthermore, a lack of degradation of apoptotic cells means that they might undergo secondary necrosis. As a result, intracellular components are released into the environment, which can affect the surrounding tissue and promote inflammatory processes. Such potentially harmful processes were demonstrated in a TREM2 knock-out mouse model (Kawabori et al., 2015). In the study, animals showed an increased number of apoptotic cells in the DG after stroke, as they were unable to produce the TREM2 receptor involved in microglial phagocytosis. These findings were associated with increased infarct size and poorer outcomes in neurological function tests.

The impact of reduced microglial activity on neurogenesis after stroke has not yet been adequately investigated. Previous data (Diaz-Aparicio et al., 2020) have already shown that microglia act as a sensor for local cell death and modulate the balance between proliferation and survival in the brain through the phagocytosis secretome and thereby maintain adult neurogenesis on the long term. On the other hand, it has been shown that inflammation triggered by the systemic application of LPS led to a reduction in the formation of new neurons in the hippocampus (Hoehn, Palmer, & Steinberg, 2005; Lindvall & Kokaia, 2015). This effect could be blocked by the administration of anti-inflammatory drugs such as indomethacin or minocycline. In this context, Luo et al. (2016) showed that following an epileptic seizure, a reduction in microglial activity after minocycline administration has a negative effect on phagocytosis activity. Fewer apoptotic cells were enclosed after minocycline administration, suggesting an increased survival of ectopic newly generated cells. It can be assumed that the reduced phagocytosis activity of the microglia after a stroke contributes to the reduction of the functional outcome.

The underlying mechanisms and the consequences of the early impaired microglial phagocytosis on functional outcome following lesion, as well as on hippocampal neurogenesis, are still not known and deserve further investigation. The extent to which the secretome of microglia is altered after stroke is still completely unclear and may be a starting point for further work to better understand the mechanism of impaired phagocytosis in general.

After stroke, the number of stem cells and precursor cells as well as the number of new neurons are drastically increased. Previous studies have shown that ischemia increases progenitor cell proliferation in the first post-ischemic week (Jin et al., 2001; Kunze et al., 2006; Takasawa et al., 2002; Zhu & Auer, 1995). As mentioned before, several mechanisms have been proposed. It has been shown

that small cortical infarcts in the adult neocortex affect the entire cortical network and induce widespread bi-hemisphere hypersensitivity (Buchkremer-Ratzmann, August, Hagemann, & Witte, 1996). This is accompanied by extensive alterations of the excitatory and inhibitory receptor function and expression (Qu et al., 1998; Que, Witte, et al., 1999; Redecker, Wang, Fritschy, & Witte, 2002). Some of these widespread changes are caused by chronic deafferentation, but also acute effects that occur within hours of the appearance of the lesions (Witte, 2000). In the present study, we analyzed the effects of stroke on microglia-mediated phagocytosis of newly generated cells during the first 10 days after lesion onset. Under physiological conditions, a continuous division of neural stem cells takes place in the DG. However, only a small proportion of the originally formed cells mature into the fully formed neuron. The majority of the cells perish in apoptotic processes within the first few days after division (Sierra et al., 2010). To demonstrate this development, BrdU was applied once. The number of BrdU-positive cells was then observed over time. In the study presented here, there was a non-significant increase in BrdU-positive cells within the control group in the first 4 days after BrdU application, followed by a significant decrease in the number of cells from Day 6 onwards. Such a decrease in newly formed cells over time was also demonstrated in a study by Steiner et al. (2004). In this study, 7-week-old C57BL/6 mice received a single BrdU application. A significant increase in BrdU-positive cells was found from Day 1 to Day 4, which dropped significantly again on Day 7, but still remained above the level of Day 1. After 28 days, the cell count had fallen below the initial level of the first measurement (Steiner et al., 2004).

In the present study, there is also an increase in newly formed, BrdU-positive cells within the stroke group compared to controls. This is more pronounced and takes place over a two-day longer period up to Day 6. This increase in neurogenesis is confirmed by the increase in the proliferation marker Ki-67, and was associated with an increased number of caspase-positive pyknotic cells. A stimulation of neurogenesis and increase in neuronal progenitor cells is well documented in the literature for the first days after ischemia (Dempsey, Sailor, Bowen, Tureyen, & Vemuganti, 2003; Jin et al., 2001; Komitova, Perfilieva, Mattsson, Eriksson, & Johansson, 2002). Already after a few hours, an increase in proliferation of type-1 stem cells can be recorded (Jin et al., 2001; Kunze et al., 2006; Takasawa et al., 2002). Within the next few days, there is a continuous increase in the newly formed cells. Depending on the study model, growth reaches a maximum after 4–11 days and then falls back to the initial level by Day 14 at the latest (Liu, Solway, Messing, & Sharp, 1998; Sharp, Liu, & Bernabeu, 2002; Takasawa et al., 2002). The significant increase in neurogenesis on Day 6 after stroke in the present study fits in well with these previous findings, although a drop to the initial level could be demonstrated by Day 10. Furthermore, the study also showed that the majority of BrdU-positive cells have the neuronal phenotype and express doublecortin. This proportion does not change significantly over the course of 10 days. In this context, previous studies have shown that the transition of the newly formed cells into the neuronal phenotype in particular triggers apoptosis and only a portion survives the transition. Several mechanisms can be considered as the cause of the increase in proliferation after stroke. Various studies have shown that excitatory signals occurring after stroke have a stimulating effect on neurogenesis (Arvidsson, Kokaia, & Lindvall, 2001; Deisseroth et al., 2004).

This effect is supported by remodeling processes in the neurons, in which the receptor composition for excitatory and inhibitory transmitters changes (Que, Schiene, Witte, & Zilles, 1999; Que, Witte, et al., 1999; Redecker et al., 2002). This is accompanied by extensive neuronal hyperexcitability extending to ipsi- and contralateral areas (Buchkremer-Ratzmann et al., 1996). In addition, the literature shows that the increased number of apoptotic cells, as it occurs after strokes, has a stimulatory influence on neurogenesis (Abdo et al., 2010; Magavi, Leavitt, & Macklis, 2000).

Further research is needed to understand the impact of the delayed microglial phagocytosis demonstrated in this study on post-ischemic neurogenesis. Previous studies showed the appearance of malformed aberrant neurons following stroke, which was associated with a reduction in cognitive function (Niv et al., 2012; Woitke et al., 2017). Since the physiological development and function of neurons is closely linked to the function of microglia, a better understanding of the relationship between these two processes could open up new therapeutic avenues to reduce cognitive impairment after stroke.

5 | CONCLUSIONS

Following a brain lesion, microglia become activated, not only at the side of the lesion, but also in regions distal to the lesion core. Activated microglia at the lesion side release cytokines and phagocytize apoptotic cells. Microglial phagocytosis is part of the tissue repair mechanisms following lesion. Interestingly, also non activated microglia under physiological conditions are able to phagocytize dead cells. For phagocytosis, three different mechanisms are discussed: (1) increased activation of phagocytic microglia, (2) increased number of engulfed apoptotic cells per microglia, and (3) increased total number of microglia. In the present study, we found that microglia were partially activated, but the total number remained unaltered. The number of engulfed apoptotic cells per microglia was also not affected. In addition, the number of phagocytic active microglia decreased significantly below the control level. Interestingly, phagocytosis of newly formed BrdU positive cells was not affected after lesion. The possible mechanisms responsible for the downregulated phagocytosis early after stroke in the hippocampus are not known. Also, the putative contribution of the impaired microglial phagocytosis of apoptotic cells to inflammatory processes after lesion, as well as its long-term impact on the formation of new neurons and cognitive functions, require further investigation. Previous studies in our lab found aberrant neurons after both small and large cortical infarcts (Niv et al., 2012). These abnormal neurons had dendritic trees reaching into the hilus. Whether microglial impairment might somehow influence the later development of aberrant neurons is also an open issue.

ACKNOWLEDGEMENTS

The authors would like to thank Julia Karius for excellent technical assistance. Open Access funding enabled and organized by Projekt DEAL.

AUTHOR CONTRIBUTIONS

Conceptualization, Silke Keiner; Data curation, Max Rudolph, Christian W. Schmeer, Madlen Günther, Florus Woitke, Carolin Kathner-Schaffert, Lina Karapetow, Julia Lindner; Formal analysis, Julia Lindner, Gustav Jirikowski; Supervision, Silke Keiner; Writing original draft, Max Rudolph, Christian W. Schmeer, Silke Keiner; statistical analysis, Max Rudolph, Thomas Lehmann, Silke Keiner; Writing review and editing, Christian W. Schmeer, Otto W. Witte, Christoph Redecker, Silke Keiner.

CONFLICT OF INTEREST STATEMENT

The authors declare that there is no conflict of interest.

DATA AVAILABILITY STATEMENT

Data sharing is not applicable to this article as no new data were created or analyzed in this study.

ORCID

Christian W. Schmeer https://orcid.org/0000-0002-2289-0126
Silke Keiner https://orcid.org/0000-0001-5225-9565

REFERENCES

Abdo, H., Derkinderen, P., Gomes, P., Chevalier, J., Aubert, P., Masson, D., … Lardeux, B. (2010). Enteric glial cells protect neurons from oxidative stress in part via reduced glutathione. *The FASEB Journal*, *24*(4), 1082–1094. https://doi.org/10.1096/fj.09-139519

Abiega, O., Beccari, S., Diaz-Aparicio, I., Nadjar, A., Laye, S., Leyrolle, Q., … Sierra, A. (2016). Neuronal hyperactivity disturbs ATP microgradients, impairs microglial motility, and reduces phagocytic receptor expression triggering apoptosis/microglial phagocytosis uncoupling. *PLoS Biology*, *14*(5), e1002466. https://doi.org/10.1371/journal.pbio.1002466

Alam, M. J., Kitamura, T., Saitoh, Y., Ohkawa, N., Kondo, T., & Inokuchi, K. (2018). Adult neurogenesis conserves hippocampal memory capacity. *The Journal of Neuroscience*, *38*(31), 6854–6863. https://doi.org/10.1523/JNEUROSCI.2976-17.2018

Arvidsson, A., Kokaia, Z., & Lindvall, O. (2001). N-methyl-D-aspartate receptor-mediated increase of neurogenesis in adult rat dentate gyrus following stroke. *The European Journal of Neuroscience*, *14*(1), 10–18. https://doi.org/10.1046/j.0953-816x.2001.01611.x

Bessis, A., Bechade, C., Bernard, D., & Roumier, A. (2007). Microglial control of neuronal death and synaptic properties. *Glia*, *55*(3), 233–238. https://doi.org/10.1002/glia.20459

Bielefeld, P., Dura, I., Danielewicz, J., Lucassen, P. J., Baekelandt, V., Abrous, D. N., … Fitzsimons, C. P. (2019). Insult-induced aberrant hippocampal neurogenesis: Functional consequences and possible therapeutic strategies. *Behavioural Brain Research*, *372*, 112032. https://doi.org/10.1016/j.bbr.2019.112032

Bird, C. M., & Burgess, N. (2008). The hippocampus and memory: Insights from spatial processing. *Nature Reviews. Neuroscience*, *9*(3), 182–194. https://doi.org/10.1038/nrn2335

Brainin, M., Tuomilehto, J., Heiss, W. D., Bornstein, N. M., Bath, P. M., Teuschl, Y., … Post Stroke Cognition Study, G. (2015). Post-stroke cognitive decline: An update and perspectives for clinical research. *European Journal of Neurology*, *22*(2), 229–238, e213-226. https://doi.org/10.1111/ene.12626

Braun, N., Kranczioch, C., Liepert, J., Dettmers, C., Zich, C., Busching, I., & Debener, S. (2017). Motor imagery impairment in postacute stroke patients. *Neural Plasticity*, *2017*, 4653256. https://doi.org/10.1155/2017/4653256

Buchkremer-Ratzmann, I., August, M., Hagemann, G., & Witte, O. W. (1996). Electrophysiological transcortical diaschisis after cortical photothrombosis in rat brain. *Stroke*, *27*(6), 1105–1109; discussion 1109-1111. https://doi.org/10.1161/01.str.27.6.1105

Ceanga, M., Keiner, S., Grunewald, B., Haselmann, H., Frahm, C., Couillard-Despres, S., … Kunze, A. (2019). Stroke accelerates and uncouples intrinsic and synaptic excitability maturation of mouse hippocampal DCX(+) adult-born granule cells. *The Journal of Neuroscience*, *39*(9), 1755–1766. https://doi.org/10.1523/JNEUROSCI.3303-17.2018

Chan, A., Magnus, T., & Gold, R. (2001). Phagocytosis of apoptotic inflammatory cells by microglia and modulation by different cytokines: Mechanism for removal of apoptotic cells in the inflamed nervous system. *Glia*, *33*(1), 87–95. https://doi.org/10.1002/1098-1136(20010101)33:1<87::aid-glia1008>3.0.co;2-s

Cunningham, C. L., Martinez-Cerdeno, V., & Noctor, S. C. (2013). Microglia regulate the number of neural precursor cells in the developing cerebral cortex. *The Journal of Neuroscience*, *33*(10), 4216–4233. https://doi.org/10.1523/JNEUROSCI.3441-12.2013

Dale, N., & Frenguelli, B. G. (2009). Release of adenosine and ATP during ischemia and epilepsy. *Current Neuropharmacology*, *7*(3), 160–179. https://doi.org/10.2174/157015909789152146

Deisseroth, K., Singla, S., Toda, H., Monje, M., Palmer, T. D., & Malenka, R. C. (2004). Excitation-neurogenesis coupling in adult neural stem/progenitor cells. *Neuron*, *42*(4), 535–552. https://doi.org/10.1016/s0896-6273(04)00266-1

Dempsey, R. J., Sailor, K. A., Bowen, K. K., Tureyen, K., & Vemuganti, R. (2003). Stroke-induced progenitor cell proliferation in adult spontaneously hypertensive rat brain: Effect of exogenous IGF-1 and GDNF. *Journal of Neurochemistry*, *87*(3), 586–597. https://doi.org/10.1046/j.1471-4159.2003.02022.x

Diaz-Aparicio, I., Paris, I., Sierra-Torre, V., Plaza-Zabala, A., Rodriguez-Iglesias, N., Marquez-Ropero, M., … Sierra, A. (2020). Microglia actively remodel adult hippocampal neurogenesis through the phagocytosis secretome. *The Journal of Neuroscience*, *40*(7), 1453–1482. https://doi.org/10.1523/JNEUROSCI.0993-19.2019

Escobar, B., Taura, P., Martinez-Palli, G., Fondevila, C., Balust, J., Beltran, J., … Garcia-Valdecasas, J. C. (2014). Stroke volume response to liver graft reperfusion stress in cirrhotic patients. *World Journal of Surgery*, *38*(4), 927–935. https://doi.org/10.1007/s00268-013-2289-x

Geibig, C. S., Keiner, S., & Redecker, C. (2012). Functional recruitment of newborn hippocampal neurons after experimental stroke. *Neurobiology of Disease*, *46*(2), 431–439. https://doi.org/10.1016/j.nbd.2012.02.007

Hoehn, B. D., Palmer, T. D., & Steinberg, G. K. (2005). Neurogenesis in rats after focal cerebral ischemia is enhanced by indomethacin. *Stroke*, *36*(12), 2718–2724. https://doi.org/10.1161/01.STR.0000190020.30282.cc

Jessberger, S., & Parent, J. M. (2015). Epilepsy and adult neurogenesis. *Cold Spring Harbor Perspectives in Biology*, *7*(12), a020677. https://doi.org/10.1101/cshperspect.a020677

Jin, K., Minami, M., Lan, J. Q., Mao, X. O., Batteur, S., Simon, R. P., & Greenberg, D. A. (2001). Neurogenesis in dentate subgranular zone and rostral subventricular zone after focal cerebral ischemia in the rat. *Proceedings of the National Academy of Sciences of the United States of America*, *98*(8), 4710–4715. https://doi.org/10.1073/pnas.081011098

Kathner-Schaffert, C., Karapetow, L., Gunther, M., Rudolph, M., Dahab, M., Baum, E., … Keiner, S. (2019). Early stroke induces long-term impairment of adult neurogenesis accompanied by hippocampal-mediated cognitive decline. *Cell*, *8*(12), 1654. https://doi.org/10.3390/cells8121654

Kawabori, M., Kacimi, R., Kauppinen, T., Calosing, C., Kim, J. Y., Hsieh, C. L., … Yenari, M. A. (2015). Triggering receptor expressed on myeloid cells 2 (TREM2) deficiency attenuates phagocytic activities of microglia and exacerbates ischemic damage in experimental stroke. *The Journal of Neuroscience*, *35*(8), 3384–3396. https://doi.org/10.1523/JNEUROSCI.2620-14.2015

Keiner, S., Walter, J., Oberland, J., & Redecker, C. (2010). Contribution of constitutively proliferating precursor cell subtypes to dentate neurogenesis after cortical infarcts. *BMC Neuroscience*, *11*, 146. https://doi.org/10.1186/1471-2202-11-146

Kim, D. H., Lee, H. E., Kwon, K. J., Park, S. J., Heo, H., Lee, Y., … Ryu, J. H. (2015). Early immature neuronal death initiates cerebral ischemia-induced neurogenesis in the dentate gyrus. *Neuroscience*, *284*, 42–54. https://doi.org/10.1016/j.neuroscience.2014.09.074

Komitova, M., Perfilieva, E., Mattsson, B., Eriksson, P. S., & Johansson, B. B. (2002). Effects of cortical ischemia and postischemic environmental enrichment on hippocampal cell genesis and differentiation in the adult rat. *Journal of Cerebral Blood Flow and Metabolism*, *22*(7), 852–860. https://doi.org/10.1097/00004647-200207000-00010

Kroemer, G., Galluzzi, L., Vandenabeele, P., Abrams, J., Alnemri, E. S., Baehrecke, E. H., … Nomenclature Committee on Cell, D. (2009). Classification of cell death: Recommendations of the Nomenclature Committee on cell death 2009. *Cell Death and Differentiation*, *16*(1), 3–11. https://doi.org/10.1038/cdd.2008.150

Kunze, A., Grass, S., Witte, O. W., Yamaguchi, M., Kempermann, G., & Redecker, C. (2006). Proliferative response of distinct hippocampal progenitor cell populations after cortical infarcts in the adult brain. *Neurobiology of Disease*, *21*(2), 324–332. https://doi.org/10.1016/j.nbd.2005.07.013

Lindvall, O., & Kokaia, Z. (2015). Neurogenesis following stroke affecting the adult brain. *Cold Spring Harbor Perspectives in Biology*, *7*(11), a019034. https://doi.org/10.1101/cshperspect.a019034

Liu, J., Solway, K., Messing, R. O., & Sharp, F. R. (1998). Increased neurogenesis in the dentate gyrus after transient global ischemia in gerbils. *The Journal of Neuroscience*, *18*(19), 7768–7778.

Luo, C., Koyama, R., & Ikegaya, Y. (2016). Microglia engulf viable newborn cells in the epileptic dentate gyrus. *Glia*, *64*(9), 1508–1517. https://doi.org/10.1002/glia.23018

Magavi, S. S., Leavitt, B. R., & Macklis, J. D. (2000). Induction of neurogenesis in the neocortex of adult mice. *Nature*, *405*(6789), 951–955. https://doi.org/10.1038/35016083

McGill, B. E., Barve, R. A., Maloney, S. E., Strickland, A., Rensing, N., Wang, P. L., … Milbrandt, J. (2018). Abnormal microglia and enhanced inflammation-related gene transcription in mice with conditional deletion of Ctcf in Camk2a-Cre-expressing neurons. *The Journal of Neuroscience*, *38*(1), 200–219. https://doi.org/10.1523/JNEUROSCI.0936-17.2017

Melani, A., Turchi, D., Vannucchi, M. G., Cipriani, S., Gianfriddo, M., & Pedata, F. (2005). ATP extracellular concentrations are increased in the rat striatum during in vivo ischemia. *Neurochemistry International*, *47*(6), 442–448. https://doi.org/10.1016/j.neuint.2005.05.014

Mijajlovic, M. D., Pavlovic, A., Brainin, M., Heiss, W. D., Quinn, T. J., Ihle-Hansen, H. B., … Bornstein, N. M. (2017). Post-stroke dementia—A comprehensive review. *BMC Medicine*, *15*(1), 11. https://doi.org/10.1186/s12916-017-0779-7

Niv, F., Keiner, S., Krishna, K., Witte, O. W., Lie, D. C., & Redecker, C. (2012). Aberrant neurogenesis after stroke: a retroviral cell labeling study. *Stroke*, *43*(9), 2468–2475. https://doi.org/10.1161/STROKEAHA.112.660977

Ojagbemi, A., & Ffytche, D. H. (2016). Are stroke survivors with delirium at higher risk of post-stroke dementia? Current evidence and future directions. *International Journal of Geriatric Psychiatry*, *31*(12), 1289–1294. https://doi.org/10.1002/gps.4506

Palomba, N. P., Martinello, K., Cocozza, G., Casciato, S., Mascia, A., Di Gennaro, G., … Fucile, S. (2021). ATP-evoked intracellular Ca(2+) transients shape the ionic permeability of human microglia from epileptic temporal cortex. *Journal of Neuroinflammation*, *18*(1), 44. https://doi.org/10.1186/s12974-021-02096-0

Popp, A., Jaenisch, N., Witte, O. W., & Frahm, C. (2009). Identification of ischemic regions in a rat model of stroke. *PLoS One*, *4*(3), e4764. https://doi.org/10.1371/journal.pone.0004764

Qu, M., Buchkremer-Ratzmann, I., Schiene, K., Schroeter, M., Witte, O. W., & Zilles, K. (1998). Bihemispheric reduction of GABAA receptor binding following focal cortical photothrombotic lesions in the rat brain. *Brain Research*, *813*(2), 374–380. https://doi.org/10.1016/s0006-8993(98)01063-4

Que, M., Schiene, K., Witte, O. W., & Zilles, K. (1999). Widespread up-regulation of N-methyl-D-aspartate receptors after focal photothrombotic lesion in rat brain. *Neuroscience Letters*, *273*(2), 77–80. https://doi.org/10.1016/s0304-3940(99)00598-4

Que, M., Witte, O. W., Neumann-Haefelin, T., Schiene, K., Schroeter, M., & Zilles, K. (1999). Changes in GABA(A) and GABA(B) receptor binding following cortical photothrombosis: A quantitative receptor autoradiographic study. *Neuroscience*, *93*(4), 1233–1240. https://doi.org/10.1016/s0306-4522(99)00197-9

Redecker, C., Wang, W., Fritschy, J. M., & Witte, O. W. (2002). Widespread and long-lasting alterations in GABA(a)-receptor subtypes after focal cortical infarcts in rats: Mediation by NMDA-dependent processes. *Journal of Cerebral Blood Flow and Metabolism*, *22*(12), 1463–1475. https://doi.org/10.1097/01.WCB.0000034149.72481.BD

Santiago, M. F., Veliskova, J., Patel, N. K., Lutz, S. E., Caille, D., Charollais, A., … Scemes, E. (2011). Targeting pannexin1 improves seizure outcome. *PLoS One*, *6*(9), e25178. https://doi.org/10.1371/journal.pone.0025178

Savill, J., & Fadok, V. (2000). Corpse clearance defines the meaning of cell death. *Nature*, *407*(6805), 784–788. https://doi.org/10.1038/35037722

Sedel, F., Bechade, C., Vyas, S., & Triller, A. (2004). Macrophage-derived tumor necrosis factor alpha, an early developmental signal for motoneuron death. *The Journal of Neuroscience*, *24*(9), 2236–2246. https://doi.org/10.1523/JNEUROSCI.4464-03.2004

Sharp, F. R., Liu, J., & Bernabeu, R. (2002). Neurogenesis following brain ischemia. *Brain Research. Developmental Brain Research*, *134*(1–2), 23–30. https://doi.org/10.1016/s0165-3806(01)00286-3

Sieber, M. W., Jaenisch, N., Brehm, M., Guenther, M., Linnartz-Gerlach, B., Neumann, H., … Frahm, C. (2013). Attenuated inflammatory response in triggering receptor expressed on myeloid cells 2 (TREM2) knock-out mice following stroke. *PLoS One*, *8*(1), e52982. https://doi.org/10.1371/journal.pone.0052982

Sierra, A., Encinas, J. M., Deudero, J. J., Chancey, J. H., Enikolopov, G., Overstreet-Wadiche, L. S., … Maletic-Savatic, M. (2010). Microglia shape adult hippocampal neurogenesis through apoptosis-coupled phagocytosis. *Cell Stem Cell*, *7*(4), 483–495. https://doi.org/10.1016/j.stem.2010.08.014

Sierra, A., Martin-Suarez, S., Valcarcel-Martin, R., Pascual-Brazo, J., Aelvoet, S. A., Abiega, O., … Encinas, J. M. (2015). Neuronal hyperactivity accelerates depletion of neural stem cells and impairs hippocampal neurogenesis. *Cell Stem Cell*, *16*(5), 488–503. https://doi.org/10.1016/j.stem.2015.04.003

Sierra-Torre, V., Plaza-Zabala, A., Bonifazi, P., Abiega, O., Diaz-Aparicio, I., Tegelberg, S., … Sierra, A. (2020). Microglial phagocytosis dysfunction in the dentate gyrus is related to local neuronal activity in a genetic model of epilepsy. *Epilepsia*, *61*(11), 2593–2608. https://doi.org/10.1111/epi.16692

Steiner, B., Kronenberg, G., Jessberger, S., Brandt, M. D., Reuter, K., & Kempermann, G. (2004). Differential regulation of gliogenesis in the context of adult hippocampal neurogenesis in mice. *Glia*, *46*(1), 41–52. https://doi.org/10.1002/glia.10337

Takasawa, K., Kitagawa, K., Yagita, Y., Sasaki, T., Tanaka, S., Matsushita, K., … Matsumoto, M. (2002). Increased proliferation of neural progenitor

cells but reduced survival of newborn cells in the contralateral hippocampus after focal cerebral ischemia in rats. *Journal of Cerebral Blood Flow and Metabolism*, *22*(3), 299–307. https://doi.org/10.1097/00004647-200203000-00007

Toda, T., Parylak, S. L., Linker, S. B., & Gage, F. H. (2019). The role of adult hippocampal neurogenesis in brain health and disease. *Molecular Psychiatry*, *24*(1), 67–87. https://doi.org/10.1038/s41380-018-0036-2

Wakselman, S., Bechade, C., Roumier, A., Bernard, D., Triller, A., & Bessis, A. (2008). Developmental neuronal death in hippocampus requires the microglial CD11b integrin and DAP12 immunoreceptor. *The Journal of Neuroscience*, *28*(32), 8138–8143. https://doi.org/10.1523/JNEUROSCI.1006-08.2008

Walter, J., Keiner, S., Witte, O. W., & Redecker, C. (2011). Age-related effects on hippocampal precursor cell subpopulations and neurogenesis. *Neurobiology of Aging*, *32*(10), 1906–1914. https://doi.org/10.1016/j.neurobiolaging.2009.11.011

Witte, O. W. (2000). Physiological basis of pathophysiological brain rhythms. *Acta Neurobiologiae Experimentalis (Wars)*, *60*(2), 289–297.

Woitke, F., Ceanga, M., Rudolph, M., Niv, F., Witte, O. W., Redecker, C., … Keiner, S. (2017). Adult hippocampal neurogenesis poststroke: More new granule cells but aberrant morphology and impaired spatial memory. *PLoS One*, *12*(9), e0183463. https://doi.org/10.1371/journal.pone.0183463

Zelano, J. (2019). Prognosis of poststroke epilepsy. *Epilepsy & Behavior*. *104*. https://doi.org/10.1016/j.yebeh.2019.04.026

Zhu, C. Z., & Auer, R. N. (1995). Graded hypotension and MCA occlusion duration: Effect in transient focal ischemia. *Journal of Cerebral Blood Flow and Metabolism*, *15*(6), 980–988. https://doi.org/10.1038/jcbfm.1995.124

SUPPORTING INFORMATION

Additional supporting information may be found online in the Supporting Information section at the end of this article.

How to cite this article: Rudolph M, Schmeer CW, Günther M, et al. Microglia-mediated phagocytosis of apoptotic nuclei is impaired in the adult murine hippocampus after stroke. *Glia*. 2021;69:2006–2022. https://doi.org/10.1002/glia.24009